Sparse Representation Based SAR Imaging Using Combined Dictionary

Han-yang Xu[1(✉)] and Feng Zhou[1,2]

[1] School of Electronic Engineering, Xidian University, Xi'an 710071, China
xhy_xidian@163.com, fzhou@mail.xidian.edu.cn
[2] National Lab of Radar Signal Processing, Xidian University, Xi'an 710071, China

Abstract. Sparse representation (SR)-based SAR imaging has shown its superior capability in high-resolution image formation. For SR-based SAR imaging task, a key challenge is how to choose a proper dictionary that can effectively represent the magnitude of the complex-valued scattering field. In this paper, we present a combined dictionary that simultaneously enhances multiple types of scattering mechanism. Trained by different kinds of SAR image patches with either strong point scatterers or smooth regions, the dictionary can represent both point-scattering and spatially distributed scenes sparsely. Finally, the SAR image is obtained by solving a joint optimization problem over the combined representation of the magnitude and phase of the observed scene.

Keywords: SAR imaging · Sparse representation · Dictionary learning
Combined dictionary

1 Introduction

Due to its day/night, all weather capabilities, synthetic aperture radar (SAR) has become one of the most promising remote sensing tools in military and civilian fields. Recently, compressive sensing (CS)-based SAR imaging has shown its superior capability in reducing sampling rate and improving image resolution compared to traditional Matched filtering (MF)-based imaging method. Baraniuk and Steeghs first demonstrated the CS theory in radar imaging in [1]. Later, Patel et al. introduced compressed SAR in [2]. Since then, CS-based SAR imaging has become a hot spot in SAR imaging community.

According to the CS theory, if the observed scene is sparse or can be sparsely represented in some space, then one can use limited radar measurements to reconstruct a high-resolution SAR image [3]. To sparsely represent the complex scene, the theory

This work was supported in part by the National Natural Science Foundation of China under Grant No. 61471284, 61522114, 61631019 and by the NSAF under Grant U1430123; it was also supported by the Young Scientist Award of Shaanxi Province under Grants 2015KJXX-19 and 2016KJXX-82.

X. Gu et al. (Eds.): MLICOM 2017, Part II, LNICST 227, pp. 124–131, 2018.
https://doi.org/10.1007/978-3-319-73447-7_15

of sparse signal reconstruction was introduced to CS-based SAR imaging. For instance, Samadi and Cetin proposed sparse representation (SR)-based SAR imaging method in [4], where the complex-valued signals were separated into real and imaginary parts to apply real-valued sparse representation methods directly to SAR imaging tasks.

In SR based SAR imaging, a key challenge is proper dictionary selection. In [4], the SR framework only focused on one type of scattering mechanism, and used common dictionaries such as discrete cosine transform (DCT) and wavelet transform coefficients. However, these dictionaries lack adaptivity in characterizing various scattering mechanisms for complex scenes.

Motivated by [5], we propose an SR-based SAR imaging method using a combined dictionary, which considers two types of most common scattering features in SAR images, i.e. strong point scatterers of man-made targets, and smooth regions of terrain or distributed natural regions. Firstly, two sub-dictionaries are trained using two types of SAR images separately. Then, we generate the third sub-dictionary by low-pass filtering for the enhancement of smooth regions. Finally, the combined-dictionary is obtained by concatenating the three sub-dictionaries, and therefore the new dictionary can represent all types of SAR scattering sparsely.

The reminder of this paper is organized as follows. Section 2 presents the framework of the proposed SAR imaging method. Section 3 shows the simulation results to verify the effectiveness of the proposed method. Section 4 provides the conclusion.

2 Framework of the Proposed SAR Imaging Method

This section describes the mathematical formulation of SR-based SAR imaging using the combined dictionary. We first introduce the observation model of SAR system and give a brief review of SR-based SAR imaging method. Then we propose our combined dictionary learning strategy. Finally, a joint iterative optimization method is presented.

2.1 SAR Observation Model

The observation geometry for spotlight SAR is shown in Fig. 1. The radar move along the straight path at constant speed v, and steers the antenna beam to the observation scene of interest. During imaging, the SAR system transmits pulses from a set of directions denoted by $\theta_k(k = 1, 2, \ldots, K$, and K is the total number of aspect angles in the azimuth dimension). The spotlight SAR transmits linear-frequency-modulated (LFM) signals $s(t) = \exp(\mathrm{j}\omega_0 t + \mathrm{j}\mu t^2)$ for $|t| \leq T_p/2$, where T_p is the pulse repetition interval, ω_0 is the carrier frequency and 2μ is the chirp rate. Assuming that the distance from radar to the scene center is much greater than the radius of ground patch, then the SAR echo $s_k(t)$ at θ_k can be described as:

$$s_k(t) = \iint\limits_{(x,y)\in D} f(x, y) \cdot \exp[-\mathrm{j}\Omega(t)(x \cos\theta_k + y \sin\theta_k)]dxdy \tag{1}$$

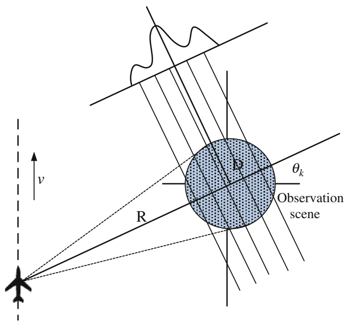

Fig. 1. SAR imaging geometry.

where D is the ground patch, (x, y) is the coordinates of scatterers in D, $f(x, y)$ is the complex-valued back-scattering coefficient at (x, y), $\Omega(t) = 2/c(\omega_0 + 2\mu(t - (2R_k/c)))$ is the radial spatial frequency, and c is the speed of light.

The imaging process can be described in a matrix form [13, 14], and the discrete observation model (1) is expressed as

$$s = \mathbf{H}f + n_0 \tag{2}$$

where s is the sampled echoes, f is the vectorized observation scene, n_0 is noise, and $\mathbf{H}$ is the SAR projection matrix containing the phase histories. For SAR imaging, the purpose is to reconstruct the unknown reflectivity f from s.

2.2 SR Based SAR Imaging

The recently emerged SR theory provides a feasible way for high-resolution SAR imaging. In an SR-based SAR imaging approach, an under-sampling strategy is carried on to the range and azimuth dimensions, and then the echo s is compressed by a sampling matrix $\mathbf{\Theta}$, so (2) can be written as:

$$y = \mathbf{\Theta}(\mathbf{H}f + n_0) = \mathbf{\Theta}\mathbf{H}f + n' \tag{3}$$

where y is the under-sampled measurements, and $n' = \mathbf{\Theta}n_0$ is the additive measurement noise. Our goal is to obtain the unknown observation scene f from the under-sampled measurements y. This ill-posed problem can be solved by a sparse signal reconstruction method. It is noticed that although f is complex-valued, we only care about its magnitude [6], thus the proposed SR-based imaging method only represents the magnitude of the complex-valued scene sparsely. In this case, we consider that:

$$\begin{aligned} & y = \mathbf{\Theta}\mathbf{H}f + n' = \mathbf{\Theta}\mathbf{H}\mathbf{P}|f| + n' \\ & S.t \quad |f| = \mathbf{\Phi}\alpha \end{aligned} \tag{4}$$

where the complex-valued scene is separated into the magnitude $|f|$ and phase matrix $\mathbf{P} = diag(\exp(j\phi_i))$. $\mathbf{\Phi}$ is a dictionary that sparsely represents the magnitude $|f|$. Given

$\mathbf{P}$, the scene f can be exactly recovered if we find a sparse coefficient α by solving the L1-norm regularization problem, i.e.

$$\hat{\alpha} = \arg\min_{\alpha}\left\{\|y - \mathbf{HP\Phi}\alpha\|_p + \lambda\|\alpha\|_1\right\} \tag{5}$$

where $\|\cdot\|_p$ is the Lp norm, and λ is the regularization parameter. In this way, the SR-based SAR imaging problem is converted to a joint optimization problem, which solves both the coefficient α and the phase matrix $\mathbf{P}$. The joint optimization approach is as follows:

(1) Using conventional MF-based SAR imaging approach to get an initial estimate of f.
(2) Given f, obtain an initial estimate of $\mathbf{P}$ using the method in [4].
(3) Solve the optimization problem in (5) and get the estimate of $|f|$ though $|f| = \mathbf{\Phi}\alpha$.
(4) Update $\mathbf{P}$ using the new estimate of $|f|$.

Since $|f|$ is real-valued, we can use the state-of-art sparse representation methods for α estimation.

This made the selection of dictionary $\mathbf{\Phi}$ a key step of SR-based SAR imaging method. The dictionary should depend on the application and the type of objects or features of interest in our observation scene.

2.3 Combined Dictionary Learning

The selection of a proper dictionary $\mathbf{\Phi}$ is a key challenge in SR-based SAR imaging. There are many useful dictionaries that can sparsely represent $|f|$. Common dictionaries generated by scaling and translation of various basis, such as Gabor and wavelet, are appropriate for wide applications. Specialized dictionaries, intended to be used with a particular class of signals, can be learned from a large dataset. For SAR imaging task, the best way to get the sparsest result is to construct an overcomplete dictionary that includes all possible scattering features. However, such dictionary may lead to severe computation problems for large area imaging. To get sufficient sparse result with limited dictionary size, we present a combined dictionary learning method using 2D wavelet image decomposing and online dictionary learning strategy.

Instead of using a general dictionary constructed by a set of basis vectors (Fourier, curvelets, etc.) or an overcomplete dictionary generated by simple shapes (points, lines and squares, etc.) [6], we consider two types of scattering features in this paper: strong point scatterers of man-made targets; and smooth regions of terrain or distributed natural regions. Such features are most common in SAR images and of particular interest in SAR imaging task. In dictionary designing, we wish to combine these two features together so that the new dictionary can represent both strong scattering points and nature smooth scenes. Since the scene to be observed is unknown, we can select a set of SAR images having the similar scattering property as a training set based on prior knowledge, and such strategy has already been proved through transfer learning [7, 8]. Then, the dictionary $\mathbf{\Phi}$ can be constructed by two sub-dictionaries. The first sub-dictionary $\mathbf{\Phi}_\mathrm{p}$ is trained by image patches with point-scattering features, such as tanks, vehicles and ships, etc., and the other sub-dictionary $\mathbf{\Phi}_r$ is trained by image patches with smooth region features, such as cropland, mountain ridge and sea surface, etc.

To reduce the dictionary size, we use 2D discrete wavelet transform (DWT) to decompose the training SAR images into multi-resolutions. Figure 2 shows the results of DWT multi-resolution decomposition of two SAR images. Figure 2(b) shows the decomposition results after 2-level DWT using Haar wavelet, and Fig. 2(c) shows the zoomed out result of subband LL3 (the small image in the top left corner of Fig. 2(b)). It can be seen that almost all the magnitude information remains in subband LL3 while other subbands contain noise and a few ignorable high-frequency components. Meanwhile, the size of subband LL3 is only a quarter of the original SAR image. Therefore, we use subband LL3 as a training sample. By this means, we reduce the dictionary size while keep the effectiveness of the dictionary. To make the dictionary more overcomplete, we also select a small part of the high-frequency components as atoms of the sub-dictionary.

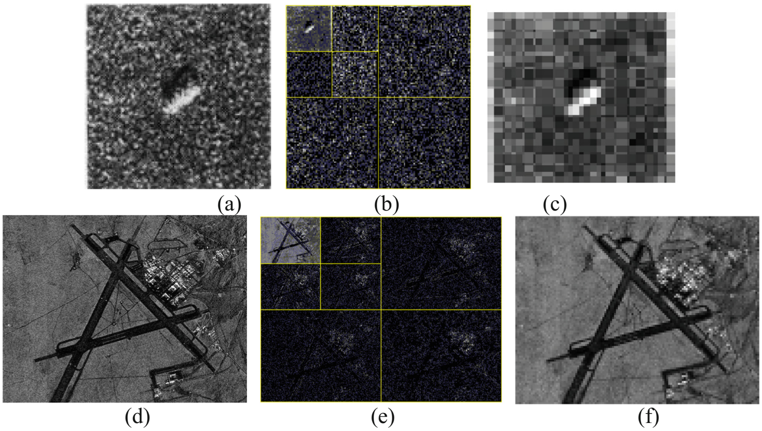

Fig. 2. 2D separable wavelet transform for SAR images. (a) original SAR images, (b) subbands after 2 level of Haar wavelet decomposition, (c) the zoom out image of subband LL3 (the small image in the top left corner of (b)), (d)–(f) results of another SAR image.

In dictionary learning, we apply the well-known recursive least squares dictionary learning algorithm (RLS-DLA). The training dataset is used iteratively to gradually improve the dictionary. Detailed information of RLS-DLA can be found in [9]. After the generation of $\mathbf{\Phi}_p$ and $\mathbf{\Phi}_r$, we add another sub-dictionary $\mathbf{\Phi}_f$, which contains several local spatial smooth filters. Particularly, each column of $\mathbf{\Phi}_f$ have the same number of elements as $\mathbf{\Phi}_p$ and $\mathbf{\Phi}_r$, with all elements set to zeroes except for a local, vectorized region around a specific pixel. $\mathbf{\Phi}_f$ can enhance the smooth regions because each atom in $\mathbf{\Phi}_f$ takes the shape of the impulse response of a low pass filter. In the proposed method, we use a set of low-pass Gaussian filters as spatial smoothing filters.

In summary, the entire dictionary is given by:

$$\mathbf{\Phi} = \left[\mathbf{\Phi}_{\mathrm{p}}, \mathbf{\Phi}_{\mathrm{r}}, \mathbf{\Phi}_{\mathrm{f}}\right] \tag{6}$$

3 Experiments

In this section, we demonstrate the validity of the proposed method. We first test the effectiveness of the proposed combined dictionary. Figure 3 visualizes the three sub-dictionaries. It can be seen that $\mathbf{\Phi}_{\mathrm{r}}$ extracts shape features such as edges and corners, and $\mathbf{\Phi}_{\mathrm{p}}$ extracts point features.

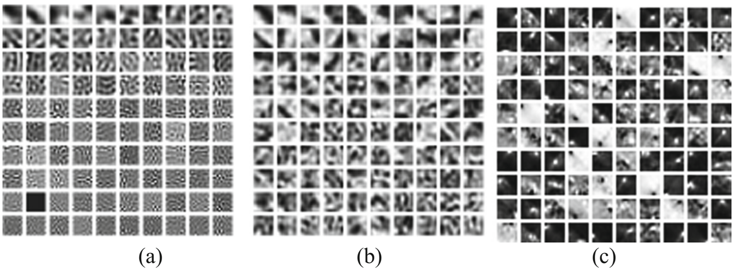

Fig. 3. Dictionary visualization. (a) Dictionary generated from randomly sampling raw training images, (b) learned sub-dictionary $\mathbf{\Phi}_{\mathrm{r}}$, (c) learned sub-dictionary $\mathbf{\Phi}_{\mathrm{p}}$.

Figure 4 shows the reconstruction error using different dictionaries. It can be seen that the proposed combined dictionary has achieved the lowest reconstruction error among other dictionaries. This is because the proposed combined dictionary can well represent all kinds of SAR images with different scattering mechanisms while other dictionaries lack completeness.

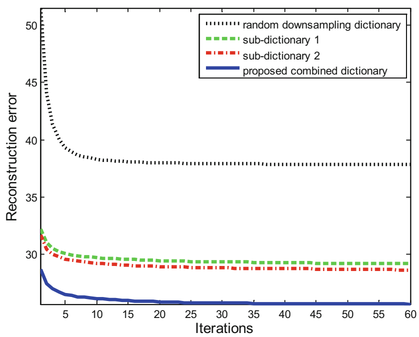

Fig. 4. Reconstruction error of different dictionaries.

Next, we test the validity of the proposed method using synthetic SAR scenes containing different kinds of scattering features. The radar parameters are shown in Table 1. We use a DCT dictionary for comparison. Figure 5 shows the final reconstructed results

Table 1. Parameters of simulated SAR system.

Carrier frequency	10 GHz
Slant range of radar center	14.14 km
Carrier frequency	10 GHz
Bandwidth	150 MHz
Pulse repetition frequency	500 Hz
Pulse repetition interval	10 us
Platform velocity	100 m/s

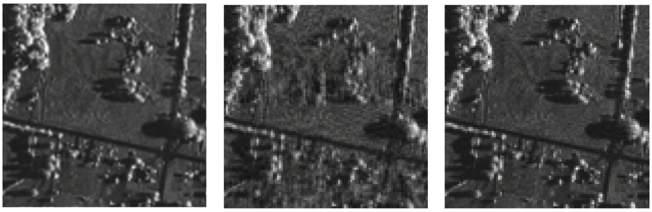
(a) (b) (c)

Fig. 5. Reconstruction of a SAR scene. (a) Observed scene, (b) reconstructed results using DCT dictionary, (c) reconstructed results using proposed combined dictionary.

Compared with the general dictionary like DCT, we see that using the proposed combined dictionary, the SR-based imaging method can suppress clutter more effectively and obtain better reconstruction result. We also use signal-to-noise ratio (SNR) and entropy of the full image (ENT) [10] for performance comparison. As is evident from Table 2, the proposed combined dictionary surpasses DCT in both SNR and ENT.

Table 2. SNR and ENT of the scene reconstructed by DCT dictionary and the proposed combined dictionary.

	DCT dictionary	Proposed combined dictionary
PSNR (dB)	28.44	31.53
ENT (dB)	0.733	0.405

4 Conclusion

In this paper, we have proposed a new approach for sparse representation based SAR imaging. Instead of using general dictionaries or single feature-based overcomplete dictionaries, we trained a combined dictionary that can enhance both strong point scattering and smooth region features. Compare to conventional dictionaries, the proposed combined dictionary can better represent the magnitude of the complex-valued scattering field. Finally, experimental results have demonstrated the validity of the proposed approach.

In the future, we intend to perform more detailed performance evaluation of our dictionary using simulated and experimental datasets.

References

1. Baraniuk, R., Steeghs, P.: Compressive radar imaging. In: Proceedings of IEEE Radar Conference, 17–20 April, Boston, MA, pp. 128–133 (2007)
2. Patel, V.M., Easley, G.R., Healy, D.M., Chellappa, R.: Compressed synthetic aperture radar. IEEE J. Sel. Topics Signal Process. **4**(2), 244–254 (2010)
3. Donoho, D.L.: Compressed sensing. IEEE Trans. Inf. Theory **30**(4), 1289–1306 (2006)
4. Samadi, S., Çetin, M., Masnadi-Shirazi, M.A.: Sparse representation based SAR imaging. IET Radar Sonar Navig. **5**(2), 182–193 (2011)
5. Samadi, S., Cetin, M., Masnadi-Shirazi, M.: Multiple feature enhanced SAR imaging using sparsity in combined dictionaries. IEEE Geosci. Remote Sens. Lett. **10**(4), 821–825 (2013)
6. Yang, J., Wright, J., Huang, T., Ma, Y.: Image super-resolution as sparse representation of raw image patches. In: Proceedings of IEEE Computer Society Conference on Computer Vision and Pattern Recognition (CVPR), 23–28 June, Anchorage, Alaska, USA, pp. 1–8 (2008)
7. Ben-David, S., Blitzer, J., Crammer, K., Pereira, F.: Analysis of representations for domain adaptation. In: Proceedings of Advances in Neural Information Processing Systems 19. MIT Press, Cambridge, pp. 137–144 (2007)
8. Luo, P., Zhuang, F.Z., Xiong, H., et al.: Transfer learning from multiple source domains via consensus regularization. In: Proceedings of the 17th ACM Conference on Information and Knowledge Management, 26–30 October, Napa Valley, California, USA, pp. 103–112 (2008)
9. Skretting, K.: Recursive least squares dictionary learning algorithm. IEEE Trans. Signal Process. **58**(4), 2121–2130 (2010)
10. Wang, J., Liu, X.: SAR minimum-entropy autofocus using an adaptive order polynomial model. IEEE Geosci. Remote Sens. Lett. **3**(4), 512–516 (2006)